Published in final edited form as:
Cardiovasc Intervent Radiol. 2013 April ; 36(2): 505–511. doi:10.1007/s00270-012-0405-1.

A comparison of direct heating during radiofrequency and microwave ablation in ex vivo liver

Anita Andreano[1] and **Christopher L Brace**[1,2]

[1]University of Wisconsin, Department of Radiology, Madison, Wisconsin

[2]Department of Biomedical Engineering, Madison, Wisconsin

Abstract

Purpose—To determine the magnitude and spatial distribution of temperature elevations when using 480 kHz RF and 2.45 GHz microwave energy in ex vivo liver models.

Materials and Methods—A total of sixty heating cycles (20 s at 90 W) were performed in normal, RF ablated and microwave ablated liver tissues (n=10 RF and n=10 microwave in each tissue type). Heating cycles were performed using a 480 kHz generator and 3 cm cooled-tip electrode (RF) or a 2.45 GHz generator and 14-gauge monopole (microwave) and designed to isolate direct heating from each energy type. Tissue temperatures were measured using fiberoptic thermosensors 5, 10 and 15 mm radially from the ablation applicator at the depth of maximal heating. Power delivered, sensor location, heating rates and maximal temperatures were compared using mixed effects regression models.

Results—No significant differences were noted in mean power delivered or thermosensor locations between RF and microwave heating groups (P>0.05). Microwaves produced significantly more rapid heating than RF at 5, 10 and 15mm in normal tissue (3.0 vs. 0.73, 0.85 vs. 0.21 and 0.17 vs. 0.09 °C/s; P<.05); and at 5 and 10mm in ablated tissues (2.3 ± 1.4 vs. 0.7 ± 0.3, 0.5 ± 0.3 vs. 0.2 ± 0.0 C/s, P<.05). The radial depth of heating was approximately 5mm greater for microwaves than RF.

Conclusions—Direct heating obtained with 2.45 GHz microwave energy using a single needle-like applicator is faster and covers a larger volume of tissue than 480 kHz RF energy. Keywords: microwave ablation, direct heating, thermal ablation

Keywords

microwave ablation; direct heating; thermal ablation

Introduction

Thermal tumor ablation is a minimally invasive therapeutic option increasingly applied to treat unresectable malignancies in a variety of organs, most commonly for primary and secondary liver tumors (1). Thermal ablation can be applied with a percutaneous approach under imaging guidance using small diameter needles with a low risk of complications and high efficacy in treating tumors up to 3-cm in diameter (2). Radiofrequency (RF) energy remains the most characterized and widely utilized heat-based ablation modality to date (1).

Address editorial correspondence to: Christopher Brace, PhD, University of Wisconsin Department of Radiology, WIMR 1141, 1111 Highland Ave. Madison, WI 53705, 608-262-4151, clbrace@wisc.edu.

Conflict of Interest Statement
Dr. Brace is a shareholder and paid consultant for NeuWave Medical.

Unfortunately, RF ablation has had limited success treating larger tumors or tumors in areas with high rates of perfusion, particularly near vessels greater than 3 mm in diameter (3–6). Some of these limitations stem from the relatively slow growth of RF ablations and a reduced ability to apply RF current through tissues with low electrical conductivity, such as the dehydrated and desiccated tissues resulting from thermal ablation, or lung and bone (7,8). Therefore, microwave energy in the range of 915 MHz to 2.45 GHz has been investigated as an alternative energy source. Microwave ablation utilizes dielectric heating around an interstitial antenna. The antenna radiates electromagnetic waves that propagate through the surrounding tissue. Energy propagation is dependent on the dielectric properties of the tissue, with more efficient propagation in tissues with lower relative permittivity or conductivity (9,10). Therefore, microwaves may be a more effective choice for heating tissues with low electrical conductivity such as lung or bone (11).

In preclinical studies, ablations produced by a 2.45 GHz microwave system were found to be larger and more reproducible than those produced by a 480 kHz RF system using single needle-like applicators (12–14). One hypothetical reason for such improved performance is that the microwave ablation system produced a larger zone of direct heating than the RF ablation system. The zone of direct heating is a volume of tissue where temperature elevations are determined predominantly by the applied energy (resistive heating for RF, dielectric heating for microwaves), rather than thermal diffusion. While a previous computer simulation study concluded that the direct heating zone produced by RF and microwave systems are not significantly different, in that study only baseline tissue conditions were considered, RF and microwave powers were not normalized, and absolute heating rates of each energy type were not compared (15). Therefore, the aim of this study was to experimentally determine the magnitude and spatial distribution of direct heating when using 480 kHz RF and 2.45 GHz microwave energy in both normal and ablated ex vivo liver tissues.

Materials and Methods

Ex vivo sample preparation

Six bovine livers were obtained from an abattoir and stored at 4°C. On the day of testing, liver sections approximately 10-cm square were warmed to room temperature (20 ± 3 °C) prior to performing the ablations. Normal tissue samples were then tested as outlined below. Ablated tissue samples were prepared by applying either microwave energy (100 W for 6 min through a monopole antenna; n = 20) or RF energy (200 W maximum, using impedance-based pulsing for 12 minutes through an internally cooled electrode; n=20) to produce an approximately 3-cm ablation zone. Ablated tissues were cooled prior to testing to eliminate variation in initial temperatures.

Temperature monitoring

A fiberoptic thermometer (FOT Lab Kit, v 2.80, Lumasense Technologies Co. Santa Clara, CA) was used to continuously measure tissue temperature during both RF and microwave heating cycles. Fiberoptic temperature sensors (model STF-2) were selected as they have negligible effect on the microwave antenna radiation pattern. Temperature values with a specified accuracy of ± 0.5 °C were recorded every second using TrueTemp software (v2.0, Lumasense Technologies Co. Santa Clara, CA). Each applicator was inserted approximately 30 mm into the tissue, and temperature probes were inserted parallel to the applicator at radial distances of 5 mm, 10 mm and 15 mm (Figure 1). The placement of the ablation applicator was planned so that temperatures were recorded from the middle of the RF electrode active length, and the base of the microwave antenna. These positions

approximately corresponded to the greatest heating rate of each device at the measurement locations, and also the largest expected ablation zone diameters.

Initial temperature of the liver was recorded as the mean temperature measured by each fiberoptic probe before the heating cycle. After the heating cycle, temperature sensors were extracted from the guide needle and replaced with plastic markers to identify the sensor position. Tissue samples were then sliced parallel to the electrode insertion track along the temperature measurement plane to record actual antenna and temperature sensor placement. Heating rates were recorded as the difference between the initial and final temperatures in each heating cycle. Using the measured heating rates, heat source terms, Q_{ext}, were also calculated from the bioheat equation by assuming that thermal diffusion was negligible by comparison, leading to the simplified relationship:

$$Q_{ext}=\rho C_p \frac{\Delta T}{\Delta t}, \quad (1)$$

where ρ is tissue density (1050 kg/m^3 in normal liver), C_p is specific heat capacity (3600 J/kg/K in normal liver), and $\Delta T/\Delta t$ is the measured heating rate (°C/s). To compare the spatial distribution of heating rates, an active heating zone was defined as the radial distance for which the calculated heat source was greater than expected heat losses from normal blood perfusion (~1 MW/m^3), assuming a perfusion rate of 1000 ml/kg/min and a required temperature elevation of 13 °C to achieve microvascular coagulation (10,16).

Tissue heating technique

After placement of the ablation applicator and temperature sensors as described above, either RF (n = 30 total) or microwave energy (n = 30 total) was applied for 20 s in normal tissue (n = 10 each energy), RF-ablated tissue (n=10 each energy), or microwave-ablated tissue (n = 10 each energy). The relatively short heating time was used to minimize thermal diffusion, allowing the more dominant effects of direct heating produced by the applied energy to be measured. RF heating cycles were performed at 90 W by using a 480 kHz generator and 17-gauge internally cooled electrode with 3 cm active length (Cooltip; Valleylab, Boulder, CO). Water-cooling was not used during heating cycles to eliminate interference with heat transfer in the tissue. Generator output current, power, impedance and electrode tip temperature were all monitored continuously during RF ablations with 10 mA, 1 W and 1 Ω and 1 °C resolution, respectively.

Microwave heating cycles were carried out using a 14-gauge monopole antenna delivering power from a 2.45 GHz generator (Cober Muegge, Norwalk, CT). Energy was delivered from the generator to the antenna through a 1.5 m-long coaxial cable and standard subminiature ‘A’ connector (RG400: Pasternack Enterprises, Irvine, CA). A generator output of 150 W was needed to offset attenuation in the cable and connectors, ensuring net power delivery of 90 W. Output power and reflected power at the generator were recorded continuously with 1 W resolution.

Statistical analysis

Heating rates and the absolute temperature rises at each measurement point were calculated. A mixed effect regression model controlled for power and distance was used to compare heating rates and absolute temperature rises in different groups. A second model was used to determine the effects of tissue and power type at each of the three measurement distances. The model included a full interaction between power and tissue type and was conducted separately by measurement distance to generate the predicted means for each energy in each tissue type. Also using a linear mixed-effects regression models, we examined whether there was evidence of a bias in temperature sensor distance between the radiofrequency and

microwaves samples. Predicted means and p-values for the comparisons are reported, with *P*-values less than 0.05 considered significant. Statistical analyses were performed using SAS, version 9.1.3 (SAS Institute Inc., Cary, NC)

Results

Ablation parameters and setup

Initial tissue temperatures, impedance before RF heating, total power delivered, final temperatures at the tip of the RF electrode, and reflected power are reported in Table I. No correlation between net power delivered and heating rate or temperature rise was found in any of the groups ($P = 0.63$). Initial impedance before RF ablations in microwave-ablated liver was significantly greater than the initial impedance in normal or RF-ablated liver ($P < 0.01$, all comparisons). No statistical difference was noted between the final tip temperatures after RF heating in any of the groups ($P = 0.09$). Mean reflected power was ~1 W greater during microwave heating in ablated liver when compared to normal liver, but this result was not statistically or practically significant ($P = 0.23$).

Sensor placements

No differences in fiberoptic temperature sensor placement were noted between RF and microwave heating setups in any tissue type ($P > 0.05$, Table II). Mean distance between the applicator and sensors at the 5 mm, 10 mm and 15 mm positions was accurate to within 1 mm, suggesting and estimated measurement error of ± 0.5 mm.

Heating rates and absolute temperature rise

Temperature elevations measured during heating cycles with each energy source and in each tissue type is noted in Figure 2. Mixed model analysis revealed that microwave heating was 2.4 times faster than RF heating when all factors were considered globally ($P < 0.0001$). In normal liver, mean heating rates were greater for microwaves than at RF at each of the 5 mm, 10 mm and 15 mm measurement positions (3.03 vs. 0.73 °C/s, 0.85 vs. 0.21 °C/s, and 0.17 vs. 0.09 °C/s, respectively; Table III). A similar result was observed when comparing microwave heating in previously microwave-ablated liver to RF heating in previously RF-ablated liver at 5 mm and 10 mm (1.84 vs. 0.69 °C/s and 0.34 vs. 0.17 °C/s, respectively). No difference was observed at 15 mm between microwave and RF heating in previously ablated tissue (0.08 vs. 0.10 °C/s).

Tissue that underwent either RF or microwave ablation was associated with a lower heating rate than the same energy modality in normal tissue ($P = 0.0433$ and $P = 0.0008$, respectively). No significant difference was observed at any distance for RF heating in normal tissue compared to RF heating in RF-ablated tissue ($P > 0.05$, all positions). However, microwave heating was less rapid in microwave-ablated tissue than in normal tissue, which was statistically significant at the 10 mm and 15 mm positions ($P < 0.05$ at 10 mm and 15 mm) but only suggestive at the 5 mm position ($P = 0.07$).

A spatial profile of RF and microwave heating rates is shown in Figure 3 along with an estimated heat sink from normal blood perfusion in the liver. RF heating exceeded the heat sink up to a radius of 9 mm, indicating a direct heating zone 18 mm in diameter. The calculated direct heating diameter for microwaves was 28 mm, or 55% greater than for RF. Similarly, we noted that the radial depth of direct microwave heating was approximately 5 mm greater than RF for any given heating source value.

Discussion

This study aimed to determine the spatial heating distribution of a fixed power (90 W) of either RF electrical current at 480 kHz or 2.45 GHz microwave energy. Both normal and previously ablated tissue media were considered. Overall, microwave heating was more rapid over a larger volume. This trend continued even in previously ablated tissue, whose electromagnetic and thermal properties reproduce a more advanced time point of the ablation process. Since the short heating time minimized thermal diffusion, it is reasonable to conclude that microwaves produce greater direct heating than RF current up to 15 mm from the applicator.

Cell death via coagulative necrosis occurs rapidly when temperatures exceed 50 °C (17). The objective of thermal ablation is to exceed this threshold throughout the tumor volume plus an ablative margin for greatest efficacy. The final ablation zone is created by a combination of what has been termed direct heating, which is heating caused directly by the applied energy source, and thermal diffusion of that heat into lower temperature tissues at the ablation periphery (15). Thermal diffusion is substantially affected by heterogeneity in blood perfusion rates and tissue properties, making it a somewhat unreliable source of temperature elevation. At the ablation zone boundary, thermal diffusion is counteracted by convection cooling due to blood flow, providing a limit to ablation zone growth (18,19). On the other hand, direct heating can be controlled by adjusting applicator design and power input to more effectively overcome blood perfusion and heat sinks, potentially creating larger ablations in shorter times. From a clinical perspective, greater direct heating may then improve the predictability and efficacy of thermal ablation. A few studies explored the degree of the heat sink phenomenon for microwave ablation in vivo animal models and noted minimal effects (20,21). The lower impact of the heat sink effect on microwave ablation compared to RF could be related not only to the larger direct heating component, but also to the higher absolute temperatures and, hence, greater total heat transfer that can be achieved with microwave energy. From a clinical perspective, greater direct heating may then improve the predictability and efficacy of thermal ablation.

Computer simulations of RF and microwave ablation have been used to evaluate the contributions of direct heating and thermal conduction on the final ablation zone (15). That study concluded that the relative contribution of direct heating was similar between energy types, with a slightly larger direct heating zone in microwave ablations. However, limitations to that study included numerical tissue models that did not account for many of the complex changes that occur during ablative heating, a lack of power control on RF ablations, and a relative comparison of heat generation and thermal diffusion for each energy type with no comparison of the absolute heating rates. The present experimental study demonstrated that when controlled for power output, the direct heating zone with microwave energy was significantly larger than for RF current.

One practical implication of this study is that maximizing the direct heating zone may create more precise microwave ablations. Antenna designs vary, with each producing a somewhat different zone of direct heating (22–24). It is possible that our results may have differed if other antenna designs, input powers, or operating frequencies were considered. Similarly, RF electrode design may have affected the reported outcomes. In this study, the applicators were chosen due to their relatively similar morphologies, which made comparison more feasible. Given the significant differences between RF and microwave heating measured in both types of tissue, and the fact that larger zones of direct heating can be realized with other microwave antenna designs, we believe the conclusions of this study would hold with other equipment as well.

A limitation of our study is the degree of variability in heating rates. Such variability is likely related to the inhomogeneity of the tissue model, especially near blood vessels, which can contain an artificially high amount of air in ex vivo. A second limitation is that this ex vivo model does not account for liver perfusion. Instead, the ex vivo model was selected to improve setup precision and reduce independent variables such as perfusion on temperature elevation. We note that the choice of heat loss used to compare RF and microwave heating zones was somewhat arbitrary; however, shifting the dashed line in Figure 3 up or down reveals that the radial depth of heating created by microwaves is approximately 5 mm greater than for RF over all heat source values. The calculation of a heat sink was intended primarily to illustrate the relative size of the RF or microwave heat source, rather than provide an exact calculation of direct heating.

RF-ablated and microwave-ablated tissues samples were used at room temperature, so did not account for temperature-dependent electrical or thermal properties, or the effects of acute water vaporization (25). Some of the effects noted in this study, such as increased RF impedance and decreased microwave heating in the desiccated tissue, could be more pronounced during ablation. Microwave ablations in RF-ablated tissue and RF ablations in microwave-ablated tissue were used only as controls, having no physical relevance to clinical scenarios. We also note that the heat source in ablated tissues was not calculated since the density and specific heat capacity of these samples were not known. Despite these limitations, we noted a greater relative decrease in heating rates in ablated samples when using microwaves. We attribute this observation to the dehydrated nature of ablated tissues. Microwaves require water and ionic fluids to generate heat. A reduction in water content would, thus, decrease microwave energy absorption and lower the heating rate in the ablated region and allow energy to flow deeper into the surrounding tissue. However, because the ablated tissue exhibited a higher impedance to RF current flow, a higher generator voltage had to be applied to maintain the 90 W output. In essence, the RF heating pattern was maintained while the microwave heating pattern became more diffuse. In-vivo, changes in heating rates may be smaller than noted here since blood perfusion may tend to keep the in vivo tissue more hydrated.

This investigation was limited to healthy liver tissue. We anticipate that similar trends would be observed in other tissue types; however, the composition of the tissue (e.g. fat or air content) may affect RF and microwave heating differently. Variability of perfusion between organs and tissue types (e.g. lung, or kidney tumors near the hilum) could also influence the relating heating rates of RF and microwave devices in each case (8–9). More study is necessary to determine how the results reported here would be affected by tissue composition.

In conclusion, our data showed that 2.45 GHz microwaves produced greater heating rates over a larger volume of tissue than the same power of 480 kHz RF current in normal and ablated liver ex vivo. This finding may help explain why larger ablation zones and less influence of blood perfusion and local heat sinks have been observed in microwave ablation studies to date.

Acknowledgments

This research was supported by grants from the National Institutes of Health.

This work was supported by grant R01 CA142737 from the National Institutes of Health.

References

1. Ahmed M, Brace CL, Lee FT Jr, Goldberg SN. Principles of and advances in percutaneous ablation. Radiology. 2011; 258(2):351–69. [PubMed: 21273519]
2. Livraghi T, Meloni F, Di Stasi M, Rolle E, Solbiati L, Tinelli C, et al. Sustained complete response and complications rates after radiofrequency ablation of very early hepatocellular carcinoma in cirrhosis: Is resection still the treatment of choice? Hepatology. 2008; 47(1):82–9. [PubMed: 18008357]
3. Lu DSK, Raman SS, Vodopich DJ, Wang M, Sayre J, Lassman C. Effect of vessel size on creation of hepatic radiofrequency lesions in pigs: assessment of the “heat sink” effect. AJR Am J Roentgenol. 2002; 178(1):47–51. [PubMed: 11756085]
4. Lu DSK, Raman SS, Limanond P, Aziz D, Economou J, Busuttil R, et al. Influence of large peritumoral vessels on outcome of radiofrequency ablation of liver tumors. J Vasc Interv Radiol. 2003; 14(10):1267–74. [PubMed: 14551273]
5. Bhardwaj N, Strickland AD, Ahmad F, Atanesyan L, West K, Lloyd DM. A comparative histological evaluation of the ablations produced by microwave, cryotherapy and radiofrequency in the liver. Pathology. 2009; 41(2):168–72. [PubMed: 19152189]
6. Kim, Y-sun; Rhim, H.; Cho, OK.; Koh, BH.; Kim, Y. Intrahepatic recurrence after percutaneous radiofrequency ablation of hepatocellular carcinoma: analysis of the pattern and risk factors. Eur J Radiol. 2006; 59(3):432–41. [PubMed: 16690240]
7. Pop M, Molckovsky A, Chin L, Kolios MC, Jewett MAS, Sherar MD. Changes in dielectric properties at 460 kHz of kidney and fat during heating: importance for radio-frequency thermal therapy. Phys Med Biol. 2003; 48(15):2509–25. [PubMed: 12953912]
8. Solazzo SA, Liu Z, Lobo SM, Ahmed M, Hines-Peralta AU, Lenkinski RE, et al. Radiofrequency ablation: importance of background tissue electrical conductivity an agar phantom and computer modeling study. Radiology. 2005; 236(2):495–502. [PubMed: 16040906]
9. Schepps JL, Foster KR. The UHF and microwave dielectric properties of normal and tumour tissues: variation in dielectric properties with tissue water content. Phys Med Biol. 1980; 25(6):1149–59. [PubMed: 7208627]
10. Duck, FA. Physical Properties of Tissue: A Comprehensive Reference Book. London: Academic Press; 1990.
11. Gillams A. Tumour ablation: current role in the kidney, lung and bone. Cancer Imaging. 2009; 9(Spec No A):S68–70. [PubMed: 19965298]
12. Wright AS, Sampson LA, Warner TF, Mahvi DM, Lee FTJ. Radiofrequency versus microwave ablation in a hepatic porcine model. Radiology. 2005; 236(1):132–9. [PubMed: 15987969]
13. Brace CL, Hinshaw JL, Laeseke PF, Sampson LA, Lee FT. Pulmonary thermal ablation: comparison of radiofrequency and microwave devices by using gross pathologic and CT findings in a swine model. Radiology. 2009; 251(3):705–11. [PubMed: 19336667]
14. Andreano A, Huang Y, Meloni MF, Lee FT, Brace CL. Microwaves create larger ablations than radiofrequency when controlled for power in ex vivo tissue. Med Phys. 2010; 37(6):2967–73. [PubMed: 20632609]
15. Schramm W, Yang D, Haemmerich D. Contribution of direct heating, thermal conduction and perfusion during radiofrequency and microwave ablation. Conf Proc IEEE Eng Med Biol Soc. 2006; 1:5013–6. [PubMed: 17946669]
16. Pennes HH. Analysis of tissue and arterial blood temperatures in the resting human forearm. J Appl Physiol. 1948; 1(2):93–122. [PubMed: 18887578]
17. Nikfarjam M, Muralidharan V, Christophi C. Mechanisms of focal heat destruction of liver tumors. J Surg Res. 2005; 127(2):208–23. [PubMed: 16083756]
18. Goldberg SN, Hahn PF, Tanabe KK, Mueller PR, Schima W, Athanasoulis CA, et al. Percutaneous radiofrequency tissue ablation: does perfusion-mediated tissue cooling limit coagulation necrosis? J Vasc Interv Radiol. 1998; 9(1 Pt 1):101–11. [PubMed: 9468403]
19. Patterson EJ, Scudamore CH, Owen DA, Nagy AG, Buczkowski AK. Radiofrequency ablation of porcine liver in vivo: effects of blood flow and treatment time on lesion size. Ann Surg. 1998; 227(4):559–65. [PubMed: 9563546]

20. Yu NC, Raman SS, Kim YJ, Lassman C, Chang X, Lu DS. Microwave liver ablation: influence of hepatic vein size on heat-sink effect in a porcine model. J Vasc Interv Radiol. 2008; 19(7):1087–92. [PubMed: 18589324]

21. Bhardwaj N, Dormer J, Ahmad F, Strickland AD, Gravante G, West K, et al. Microwave ablation of the liver: a description of lesion evolution over time and an investigation of the heat sink effect. Pathology. 2011; 43(7):725–31. [PubMed: 22027742]

22. Bertram JM, Yang D, Converse MC, Webster JG, Mahvi DM. A review of coaxial-based interstitial antennas for hepatic microwave ablation. Crit Rev Biomed Eng. 2006; 34(3):187–213. [PubMed: 16930124]

23. Brace CL. Dual-slot antennas for microwave tissue heating: parametric design analysis and experimental validation. Med Phys. 2011; 38(7):4232–40. [PubMed: 21859025]

24. Cavagnaro M, Amabile C, Bernardi P, Pisa S, Tosoratti N. A minimally invasive antenna for microwave ablation therapies: design, performances, and experimental assessment. IEEE Trans Biomed Eng. 2011; 58(4):949–59. [PubMed: 21172749]

25. Ji Z, Brace CL. Expanded modeling of temperature-dependent dielectric properties for microwave thermal ablation. Phys Med Biol. 2011; 56(16):5249–64. [PubMed: 21791728]

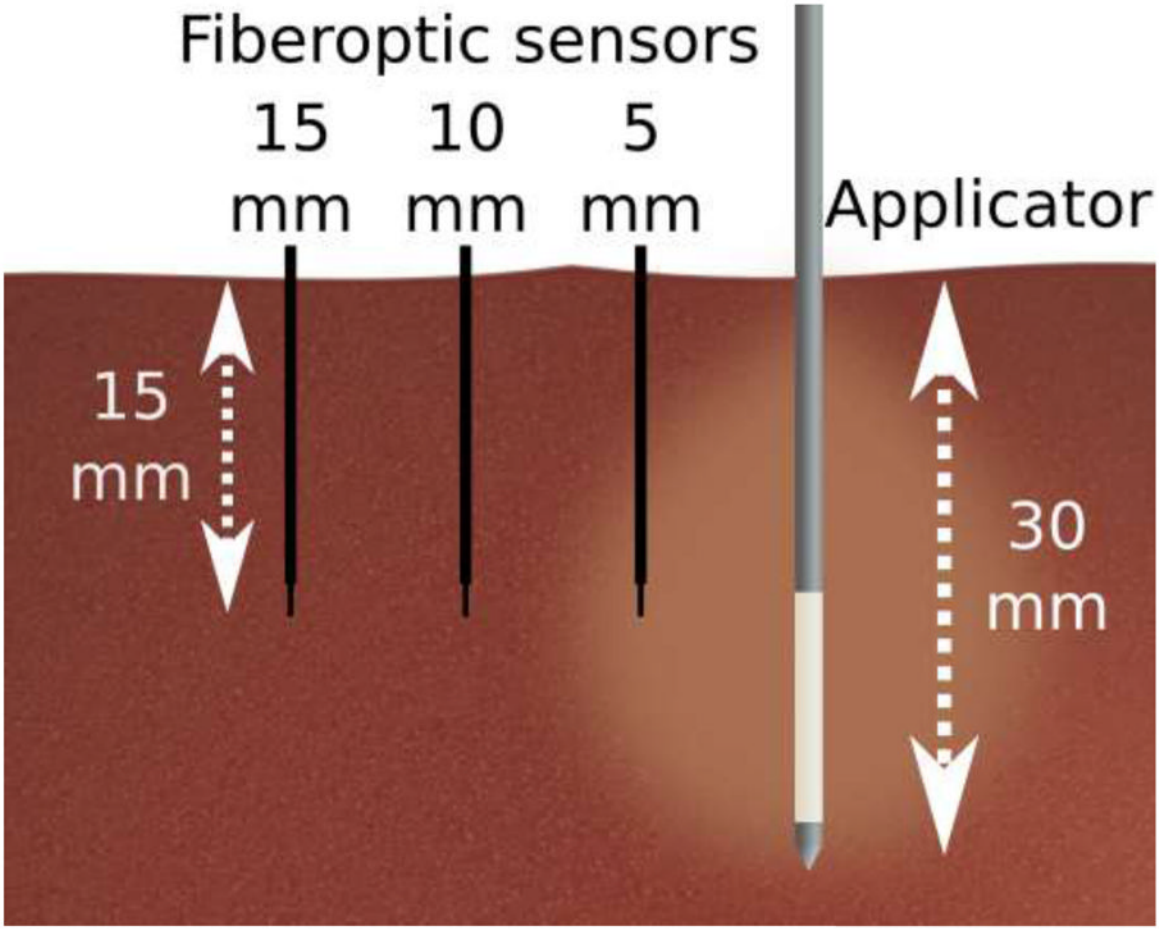

Figure 1.
Illustration of the experimental set-up. Fiberoptic temperature sensors were placed 5 mm, 10 mm and 15 mm from the applicator at a depth near the middle of the active component of the RF electrode or microwave applicator.

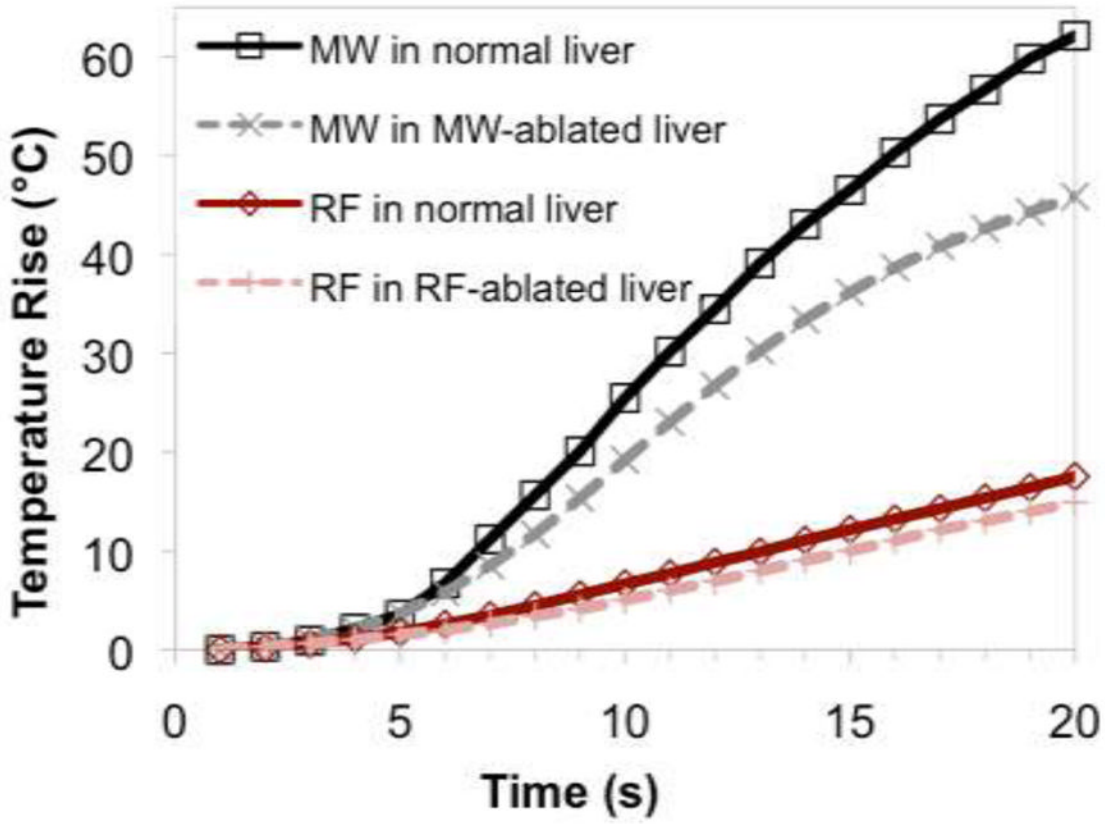

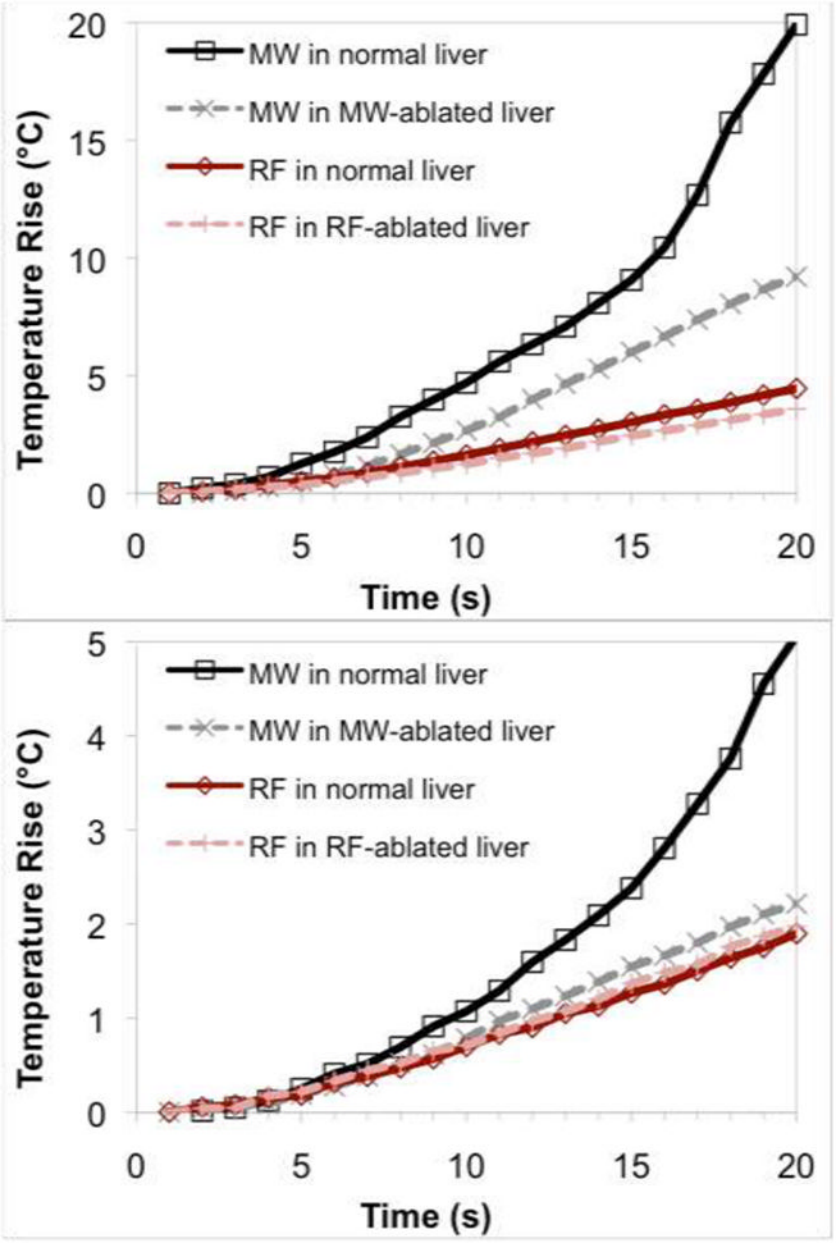

Figure 2.
Mean temperatures over time for each energy and tissue type at (a) 5 mm, (b) 10 mm and (c) 15 mm measurement locations. Microwaves provided a statistically significant increase in heating rates overall.

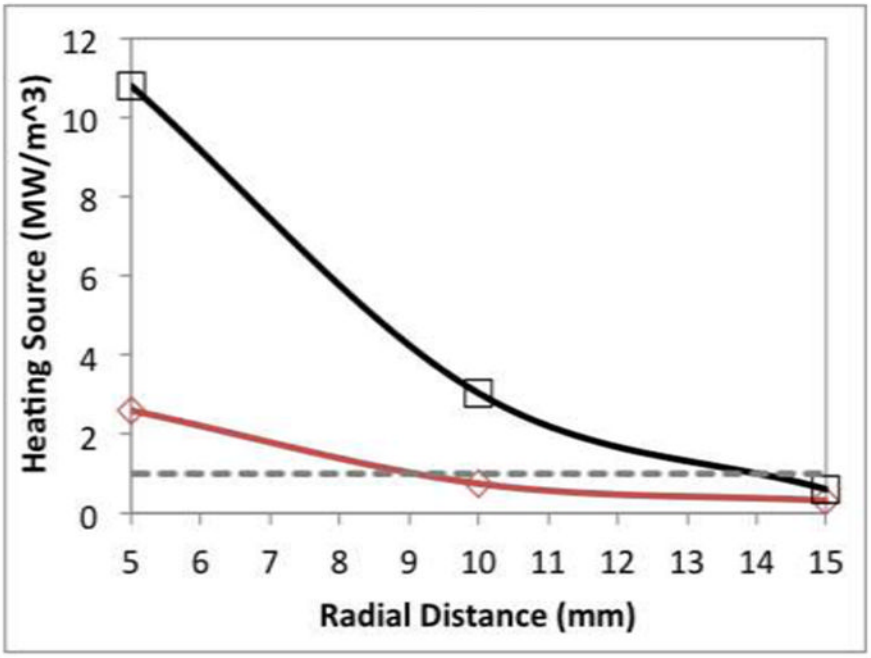

Figure 3.
Heat source calculated at each position in normal liver. The dashed line indicates a theoretical heat loss of 1.0 MW/m^3 associated with 1000 ml/kg/min blood perfusion.

Table I

Experimental design and tissue parameters. Values are given as mean ± standard deviation.

Group	Energy	Tissue	N	Initial temperature (°C)	Initial impedance (Ω)	Power Delivered (W)	Final Tip Temperature (°C)	Reflected Power (W)
1	RF	Normal liver	10	20.3 ± 1.8	78 ± 7	90.9 ± 5.7	41.5 ± 3.3	-
2	MW	Normal liver	10	20.2 ± 2.1	-	91.9 ± 4.6	-	0.2 ± 0.2
3	RF	RF- ablated liver[+]	10	20.8 ± 1.8	78 ± 12	87.4 ± 9.9	45.6 ± 4.4	-
4	MW	RF- ablated liver[+]	10	18.8 ± 1.2	-	93.3 ± 3.8	-	1.3 ± 2.3
5	RF	MW- ablated liver[*]	10	21.5 ± 1.5	103 ± 22	90.8 ± 3.8	42.5 ± 4.8	-
6	MW	MW- ablated liver[*]	10	18.5 ± 1.4	-	93.6 ± 2.2	-	1.1 ± 1.2

[+] Preparatory RF ablations were performed with a maximum of 200 W using impedance-based pulsing for 12 min.

[*] Preparatory microwave ablations were performed with 100 W for 6 min.

Cardiovasc Intervent Radiol. Author manuscript; available in PMC 2014 April 01.

Table II

Distances measured between each fiberoptic temperature sensor and the ablation applicator. Data are reported as mean ± standard deviation.

Energy	Tissue	5 mm	10 mm	15 mm
RF	Normal liver	4.8 ± 0.9	10.0 ± 1.9	14.8 ± 2.2
MW	Normal liver	5.4 ± 0.5	9.9 ± 0.9	15.0 ± 1.4
RF	RF-ablated liver	5.2 ± 0.7	10.4 ± 1.2	15.2 ± 1.3
MW	RF-ablated liver	5.4 ± 0.7	10.5 ± 1.2	15.8 ± 1.8
RF	MW-ablated liver	5.8 ± 0.9	10.7 ± 1.0	16.1 ± 1.1
MW	MW-ablated liver	5.1 ± 1.4	10.3 ± 1.5	15.0 ± 1.4

Table III

Mean heating rates for each energy type in relevant tissues. Microwaves tend to heat tissue faster both in normal tissue and in previously ablated tissues that simulate a more advanced ablation stage.

Position	Mean heating rate (°C/s)		P-value	Mean heating rate (°C/s)	
	RF	MW		RF in RF-ablated tissue	MW in MW-ablated tissue
5 mm	0.73	3.03	<0.0001	0.69	1.84
10 mm	0.21	0.85	0.0001	0.17	0.34
15 mm	0.09	0.17	0.0144	0.10	0.08